

Electron-density dependence of longitudinal-optical phonon lifetime in InN studied by subpicosecond time-resolved Raman spectroscopy

This article has been downloaded from IOPscience. Please scroll down to see the full text article.

2007 J. Phys.: Condens. Matter 19 236219

(<http://iopscience.iop.org/0953-8984/19/23/236219>)

View [the table of contents for this issue](#), or go to the [journal homepage](#) for more

Download details:

IP Address: 129.252.86.83

The article was downloaded on 28/05/2010 at 19:10

Please note that [terms and conditions apply](#).

Electron-density dependence of longitudinal-optical phonon lifetime in InN studied by subpicosecond time-resolved Raman spectroscopy

K T Tsen¹, Juliann G Kiang², D K Ferry³, Hai Lu⁴, William J Schaff⁴,
Hon-Way Lin⁵ and Shangjr Gwo⁵

¹ Department of Physics and Astronomy, Arizona State University, Tempe, AZ 85287, USA

² Scientific Research Department, Armed Forces Radiobiology Research Institute, and Department of Medicine and of Pharmacology, Uniformed Services University of The Health Sciences, Bethesda, MD 20889-5603, USA

³ Department of Electrical Engineering, Arizona State University, Tempe, AZ 85287, USA

⁴ Department of Electrical and Computer Engineering, Cornell University, Ithaca, NY 14853, USA

⁵ Department of Physics, National Tsing-Hua University, Hsin-Chu 300, Taiwan, Republic of China

Received 17 April 2007, in final form 22 April 2007

Published 15 May 2007

Online at stacks.iop.org/JPhysCM/19/236219

Abstract

Subpicosecond time-resolved Raman spectroscopy has been used to measure the lifetime of the $A_1(\text{LO})$ and $E_1(\text{LO})$ phonon modes in InN at $T = 10$ K for photoexcited electron–hole pair density ranging from 5×10^{17} to $2 \times 10^{19} \text{ cm}^{-3}$. The lifetime has been found to decrease from 2.2 ps at the lowest density to 0.25 ps at the highest density. Our experimental findings demonstrate that the carrier-density dependence of LO phonon lifetime is a universal phenomenon in polar semiconductors.

1. Introduction

New developments in crystal growth techniques have recently produced high-quality, single-crystal InN that has a band gap of about 0.7 eV at room temperature [1–5]. This indicates that its ternary compound $\text{In}_x\text{Ga}_{1-x}\text{N}$ not only has great potential for white-light generation but also is suitable for applications in solar cells. InN also has been theoretically predicted [6–8] and experimentally demonstrated [9, 10] to have enormously large transient electron drift velocity. As a result, InN is also very attractive for use in the fabrication of electronic devices of extremely high performance. A large non-equilibrium phonon population created in a semiconductor under the relaxation of carriers after excitation by an intense laser pulse, in particular with the application of an electric field, not only causes a decrease of energy loss rate of the electronic system (the so-called ‘hot-phonon effects’) but also reduces the electron drift velocity. These have been demonstrated and well understood in a variety of semiconductors such as GaAs and Si [11]. However, for some not so well established semiconductors, a case

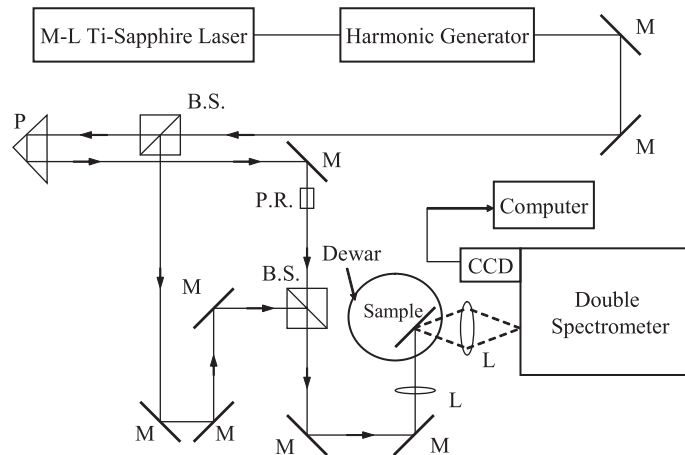


Figure 1. The experimental setup used for subpicosecond time-resolved Raman measurements of LO phonons in GaN. M: mirror; BS: beam splitter; P: prism; PR: polarization rotator; L: lens; CCD: charge-coupled device.

in point being GaN, the effects of the presence of a large non-equilibrium phonon population are less well understood, and sometimes the results are even contrary to our general belief.

The accumulation of a large non-equilibrium phonon population is a result of efficient electron–longitudinal-optical (LO) phonon coupling and a relatively long phonon lifetime. In this paper, we have systematically measured the lifetime of LO phonons in InN for a range of photoexcited electron–hole pair densities by subpicosecond time-resolved Raman spectroscopy. We find that the lifetimes of both the $A_1(\text{LO})$ and $E_1(\text{LO})$ phonon modes are reduced with increasing carrier density, in a direct and systematic manner.

2. Samples and experimental approach

The sample studied in this work is a thick InN film grown on a hydride vapour-phase epitaxy (HVPE) GaN template by the conventional molecular beam epitaxy (MBE) technique [12]. RF-remote plasma nitrogen was supplied by an EPI Unibulb source operating at 260 W with 0.7 sccm nitrogen flow. Prior to InN growth, the substrate was directly heated to 525 °C, measured by a thermocouple; then InN growth was started. The InN growth rate was about $0.7 \mu\text{m h}^{-1}$ with final film thickness around $7.5 \mu\text{m}$. The HVPE GaN template was compensated with Zn introduced during growth to suppress unintentional n-type conductivity. Its thickness was around $16 \mu\text{m}$ with 300 K resistivity up to $10^9 \Omega \text{ cm}$ and dislocation density around $5 \times 10^8 \text{ cm}^{-2}$. The resulting InN film is n-type and has an electron density of $\approx 3.5 \times 10^{17} \text{ cm}^{-3}$ and Hall mobility $2160 \text{ cm}^2 \text{ V}^{-1} \text{ s}^{-1}$ at $T = 300 \text{ K}$, as determined by Hall measurements.

The experimental technique (time-resolved Raman spectroscopy) employed in this work has been described in detail elsewhere [13, 14]. As shown in figure 1, the output of the second harmonic generation of a mode-locked Ti–sapphire laser is used as both the excitation and probing sources in our pump/probe experiments. The laser can provide a continuous pulse train of 80 MHz in repetition rate, at photon wavelengths ranging from 350 to 450 nm, having pulse width of about 100 fs and with average power of about 100 mW. The Raman signal is collected and analysed by a standard computer-controlled Raman system which includes a double spectrometer, a photomultiplier tube/CCD and their associated photon-counting electronics.

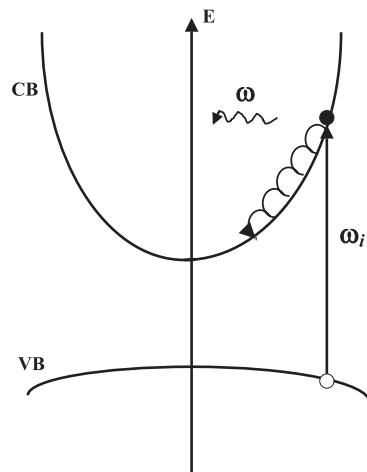


Figure 2. A diagram demonstrating how the non-equilibrium LO phonons in GaN are created. Electron–hole pairs are generated by the excitation laser pulse in a direct band gap semiconductor. The non-equilibrium LO phonons are emitted during the relaxation of energetic carriers. CB: conduction band; VB: valence band; E: energy; ω : LO phonon energy; ω_i : excitation photon energy.

All the experimental data were taken at $T = 10$ K and with the laser operating at a wavelength of 442 nm. We estimate that the penetration depth at the laser excitation wavelength is about 500 Å. In the pump/probe configuration, the ultrashort pulse train was split into two beams of equal intensity but different polarization. An appropriate analyser was placed in front of the entrance of the spectrometer so that scattered light from the pump pulse was minimized while that from the probe pulse was passed on to the detector. The photoexcited electron–hole pair density was estimated from the average laser power, focused spot size on the sample surface and the absorption depth at the excitation laser wavelength. The zero delay at the sample was determined to within ± 0.01 ps by the observance of the interference effect which occurs when the pump and probe pulses are spatially and temporally overlapped.

Figure 2 demonstrates how the non-equilibrium LO phonons were generated [15]. Electron–hole pairs are photoexcited by the excitation photons in the pump beam across the band gap of InN, which has a band gap of about 0.8 eV at $T = 10$ K. The energetic electron–hole pairs having an excess energy of about 2.01 eV will rapidly relax to the bottom of the conduction band (for electrons) and to the top of the valence band (for holes) by emitting non-equilibrium phonons through electron/hole–phonon interaction. In InN, the effective masses for the electron and hole are $m_e^* \simeq 0.14 m_e$ [16], $m_h^* \simeq 1.63 m_e$ [17], respectively, where m_e is the electron mass. As a result, most of the excess energy is distributed to the electron in the photoexcitation process. In fact, the excess energy of a hole is about 12 times smaller than that of an electron. Consequently, the contribution of holes to the generation of non-equilibrium LO phonons detected in our Raman scattering experiment is negligible in comparison with that of electrons. For a polar semiconductor such as InN, the strength of the Fröhlich interaction mechanism is much greater than that of any deformation potential mechanism [18]. As a result, these energetic carriers will relax by emitting LO phonons. By monitoring the occupation number of these emitted non-equilibrium phonons with the probe beam, information such as the strength of electron–phonon interactions can be readily obtained.

One important advantage of probing non-equilibrium excitations with Raman spectroscopy in semiconductors is that since it detects a Raman signal only when excitation photons are

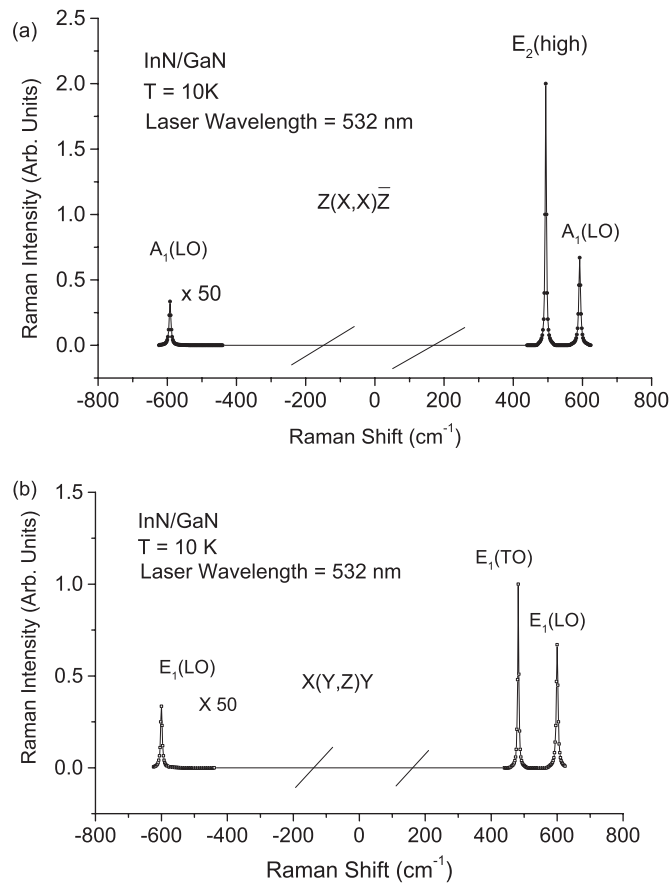


Figure 3. Typical Raman spectra of the InN sample, taken at $T = 10$ K, for two scattering configurations: (a) $X(Y, Z)Y$ and (b) $Z(X, X)\bar{Z}$, respectively; the spectra are excited by the second harmonic output of a cw mode-locked YAG laser. For clarity, the spectra for the $X(Y, Z)Y$ scattering configuration have been shifted vertically.

present, the time resolution is essentially limited by the pulse width of the excitation laser and not by the response of the detection system. This explains why our detection system has a time resolution of the order of a nanosecond, whereas the time resolution in our Raman experiments is typically on the subpicosecond scale.

3. Experimental results and analysis

Since our excitation laser has a pulse width of $\text{FWHM} \cong 120 \text{ cm}^{-1}$, whereas the energy difference between the $A_1(\text{LO})$ and $E_1(\text{LO})$ phonon modes is about 7 cm^{-1} , we need to find a way to separate the contributions of the $A_1(\text{LO})$ phonons from those of the $E_1(\text{LO})$ phonons in our time-resolved Raman experiments. Figures 3(a) and (b) show typical Stokes and anti-Stokes Raman scattering spectra of the sample taken for two scattering configurations: $X(Y, Z)Y$ and $Z(X, X)\bar{Z}$, as indicated, at $T = 10$ K using the second harmonic of a cw mode-locked YAG laser. The excitation laser has a pulse width of about 70 ps and a spectral width of $\cong 1 \text{ cm}^{-1}$. Here, $X = (100)$, $Y = (010)$ and $Z = (001)$. The Raman modes

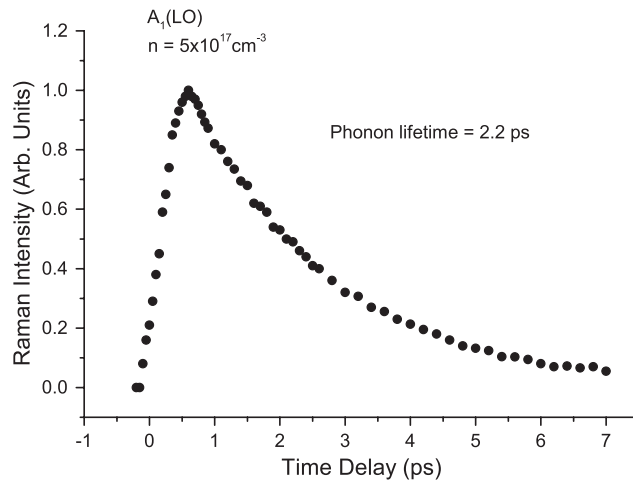


Figure 4. Integrated Raman intensity of the $A_1(\text{LO})$ phonon as a function of the delay time for an InN sample, with photoexcited electron–hole pair density of $n \approx 5 \times 10^{17} \text{ cm}^{-3}$. The deduced lifetime of the LO phonon is found to be (2.2 ± 0.2) ps.

are identified with the help of the Raman selection rules for wurzite semiconductors [19]; namely, in the $X(Y, Z)Y$ scattering configuration, the peak at 482 cm^{-1} corresponds to the $E_1(\text{TO})$ phonon mode, while the Raman signal at 599 cm^{-1} represents the $E_1(\text{LO})$ phonon mode. In the $Z(X, X)\bar{Z}$ scattering geometry, the Raman peak at 494 cm^{-1} is due to scattering of light by $E_2(\text{high})$ phonons and that at 592 cm^{-1} belongs to $A_1(\text{LO})$ phonons. At very low temperatures, the equilibrium phonon occupations are vanishingly small for these high-frequency phonon modes. The observation of LO phonon modes on the anti-Stokes side of Raman spectra at such low temperatures as $T = 10 \text{ K}$ indicates that energetic electrons relax towards the bottom of the conduction band primarily by emitting LO phonons, and driving these modes out of equilibrium. The most important aspect of these spectra is that, under the $X(Y, Z)Y$ scattering configuration, only the $E_1(\text{LO})$ phonon mode contributes to the anti-Stokes signal, whereas, under the $Z(X, X)\bar{Z}$ geometry, only the $A_1(\text{LO})$ phonon mode contributes. This intriguing aspect will be used in our time-resolved Raman experiments to measure the strength of electron–phonon interactions for the $E_1(\text{LO})$ and $A_1(\text{LO})$ phonons, by the cw mode-locked Ti–sapphire laser. In other words, we use the $Z(X, X)\bar{Z}$ scattering configuration for the $A_1(\text{LO})$ phonons and $X(Y, Z)Y$ for the $E_1(\text{LO})$ phonons.

A typical integrated anti-Stokes Raman intensity for the $A_1(\text{LO})$ phonon mode, as a function of time delay, and with a photoexcited electron–hole pair density $n \approx 5 \times 10^{17} \text{ cm}^{-3}$, is shown in figure 4. The very rapid rise of the signal from around $\Delta t = 0$ is a manifestation of an extremely large electron–LO phonon interaction in InN. It reaches a maximum at about 600 fs, indicative of the fact that, at such a time delay, electrons are no longer emitting LO phonons that are detectable by our Raman spectroscopy. After about 600 fs, the anti-Stokes Raman intensity decreases with a decay constant of $\tau = (2.2 \pm 0.2)$ ps. This we define as the population relaxation time or lifetime of the $A_1(\text{LO})$ phonon mode. The most likely decay channel for this phonon mode has been suggested previously by Tsen *et al* [20] to be a process in which a zone-centre $A_1(\text{LO})$ phonon decays into a large-wavevector TO and a large-wavevector TA/LA phonon.

Similar experiments have been performed on the GaN sample with a range of photoexcited electron–hole pair densities by varying the spot size of the excitation laser. We have found that

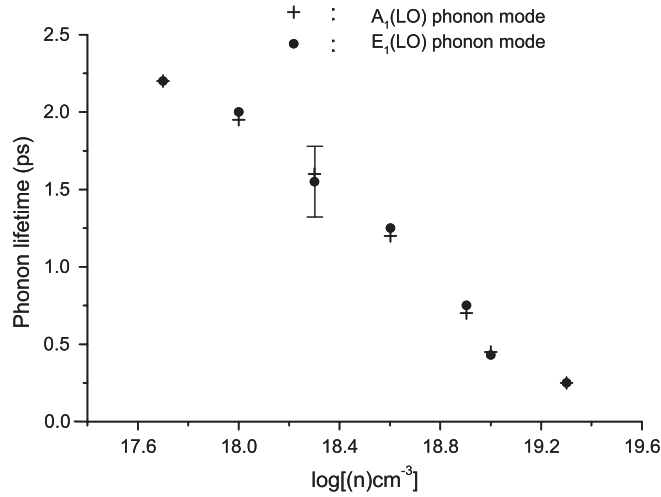


Figure 5. Phonon lifetime as a function of the photoexcited electron–hole pair density for the $A_1(\text{LO})$, $E_1(\text{LO})$ phonon modes, respectively. The error bar (± 0.25 ps) indicates the uncertainty in the measured LO phonon lifetime resulting from the possible effect of laser heating. The lifetime has been found to decrease dramatically with increasing electron–hole pair density.

the effective temperatures of non-equilibrium LO phonons at the peak of their population range from about 500 to 800 K.

It is well known [21] that the electron plasmon couples strongly with the LO phonon mode in polar semiconductors, in particular, for a plasma density greater than $5 \times 10^{17} \text{ cm}^{-3}$. We refer to the phonon-like plasmon–LO phonon coupled mode at high electron densities as the LO phonon mode. Figure 5 shows the measured lifetime of this LO phonon mode in InN as a function of the photoexcited electron–hole pair density, ranging from 5×10^{17} to $2 \times 10^{19} \text{ cm}^{-3}$ for the $A_1(\text{LO})$ and $E_1(\text{LO})$ phonon modes. The results for these two phonon modes are very similar. We observe that the lifetime of these LO phonon modes decreases from 2.2 ps to about 0.25 ps. We notice that similar observations for GaAs and GaN have been reported by Kash *et al* [22, 23] and Tsen *et al* [24], respectively, for which the physical interpretation remains unclear. Figure 5 also shows corresponding results for the $E_1(\text{LO})$ phonon mode. Again, a dramatic decrease of the lifetime of the $E_1(\text{LO})$ phonons is observed, but this decrease is commensurate with that of the $A_1(\text{LO})$ phonon mode.

The local heating due to the laser pumping will introduce some uncertainty in the experimental data. We have used the ratio of Stokes/anti-Stokes intensities of both the E_2 and $A_1(\text{TO})$ phonon modes (which do not couple to plasmon) as an indicator for the effective lattice temperature at the laser excitation spot. We have found that the effective lattice temperature is $T_{\text{eff}} \leq 100$ K, within our experimental accuracy. Since the lifetimes of LO phonons measured at an electron–hole pair density of $1 \times 10^{16} \text{ cm}^{-3}$ in InN are about 2.5 ps and 2.0 ps, for lattice temperatures at 10 K, 100 K, respectively [20], this uncertainty transforms to an uncertainty of ± 0.25 ps in the lifetime of LO phonons in our experimental data.

Our experimental results indicate that the decrease of the $E_1(\text{LO})$ phonon lifetime with increasing carrier density is commensurate with that of the $A_1(\text{LO})$ phonons. We believe that it is very likely related to the coupling strength of these LO phonon modes to the plasmon. The observed commensuration suggests that the coupling strength of the $A_1(\text{LO})$ phonon mode is about the same as that of the $E_1(\text{LO})$ phonon mode.

In general, the lifetime is dominated by the decay of the LO phonons into a pair of acoustic phonons, as discussed above. This is generally a relatively slow process, and cannot explain the density dependence. Moreover, screening cannot be invoked as a higher density would provide more screening and a slower response, opposite to that observed. However, Matulionis has suggested that the hot LO phonons can emit a plasmon in the relaxation process [25]. While intriguing, the mechanism for the decay via both plasmon and acoustic phonon modes has not yet been worked out. In particular, if the observed A_1 (LO) mode is already a coupled mode of the phonon and plasmon, it is not immediately clear how a distinct, and separate, plasmon can subsequently be emitted in the decay process. Thus, more work is needed in order to understand the mechanism by which the phonon lifetime varies with carrier density.

4. Conclusion

Subpicosecond time-resolved Raman spectroscopy has been used to measure the lifetime of the LO phonon modes in InN by photoexcited electron–hole pair creation, which subsequently produces a non-equilibrium phonon population. We have measured the resulting phonon lifetime for a density ranging from 5×10^{17} to $2 \times 10^{19} \text{ cm}^{-3}$. The lifetime has been found to decrease from 2.2 to 0.25 ps for both the A_1 (LO) and E_1 (LO) modes. Previous measurements in GaAs and GaN have also shown such a density dependence, and the present experimental findings demonstrate that carrier density dependence of the LO phonon lifetime is a likely universal phenomenon in polar semiconductors. The cause of such a density dependence is not currently understood, and more work is needed.

Acknowledgments

This work is supported by the National Science Foundation under Grant No. DMR-0305147. The work at Cornell University is supported by ONR contract No. N000149910936 monitored by Dr Colin Wood and an LBNL subcontract No. 6703635. The latter authors also want to acknowledge the technical assistance from Mark Little and Troy Richardson. Shangir Gwo would like to thank NRC of Taiwan for support. The opinions or assertions contained herein are the private views of the authors and are not to be construed as official or reflecting the views of the Armed Forces Radiobiology Research Institute, Uniformed Services University of the Health Sciences, or the US Department of Defense. The authors would also like to thank Professors Steve Goodnick and Arvydas Matulionis for helpful discussions.

References

- [1] Inushima T, Mamutin V V, Vekshin V A, Ivanov S V, Sakon T, Motokawa M and Ohoya S 2001 *J. Cryst. Growth* **227/228** 481
- [2] Davydov V Yu *et al* 2002 *Phys. Status Solidi* b **229** R1
Davydov V Yu *et al* 2002 *Phys. Status Solidi* b **230** R4
Davydov V Yu *et al* 2002 *Phys. Status Solidi* b **234** 787
- [3] Wu J, Walukiewicz W, Yu K M, Ager J W III, Haller E E, Lu H, Schaff W J, Saito Y and Nanishi Y 2002 *Appl. Phys. Lett.* **80** 3967
- [4] Wu J, Walukiewicz W, Yu K M, Ager J W III, Haller E E, Lu H and Schaff W J 2002 *Appl. Phys. Lett.* **80** 4741
- [5] Yamamoto A, Sugita K, Takatsuka H, Hashimoto A and Davydov V Yu 2004 *J. Cryst. Growth* **261** 275
- [6] O'Leary S K, Foutz B E, Shur M S, Bhapkar U V and Eastman L F 1998 *J. Appl. Phys.* **83** 826
- [7] Bellotti E, Doshi B K, Brennan K F, Albrecht J D and Ruden P P 1999 *J. Appl. Phys.* **85** 916
- [8] Foutz B E, O'Leary S K, Shur M S and Eastman L F 1999 *J. Appl. Phys.* **85** 7727
- [9] Liang W, Tsen K T, Ferry D K, Lu H and Schaff W J 2004 *Appl. Phys. Lett.* **84** 3681

- [10] Tsen K T *et al* 2005 *Superlatt. Microstruct.* **38** 77
- [11] For a review, see Shah J 1996 *Ultrafast Spectroscopy of Semiconductors and Semiconductor Nanostructures* (New York: Springer) pp 161–224
- [12] Lu H, Schaff W J, Eastman L F, Wu J, Walukiewicz W, Look D C and Molnar R J 2003 *Proc. Mater. Res. Soc. Symp.* **743** L4
- [13] Tsen K T, Kiang J G, Ferry D K and Morkoc H 2006 *Appl. Phys. Lett.* **89** 112111
- [14] Grann E D, Tsen K T, Ferry D K, Salvador A, Botcharev A and Morkoc H 1997 *Phys. Rev. B* **56** 9539
- [15] Tsen K T 2001 Ultrafast physical processes in semiconductors *Semiconductors and Semimetals* vol 67, ed K T Tsen (Boston, MA: Academic) pp 109–49
- [16] Kasic A, Schubert M, Saito Y, Nanishi Y and Wagner G 2002 *Phys. Rev. B* **65** 115206
- [17] Xu Y N and Ching W Y 1993 *Phys. Rev. B* **48** 4335
- [18] Conwell E M 1967 *High Field Transport in Semiconductors* (New York: Academic)
- [19] Harima H 2002 *J. Phys.: Condens. Matter* **14** R967
- [20] Tsen K T, Kiang J G, Ferry D K, Lu H, Schaff W J, Lin H-W and Gwo S 2007 *Appl. Phys. Lett.* **90** 152107
- [21] Abstreiter G, Cardona M and Pinczuk A 1986 *Light Scattering in Solids IV* ed M Cardona and G Güntherodt (New York: Springer) p 5 and references therein
- [22] Kash J A and Tsang J C 1988 *Solid State Electron.* **31** 419
- [23] Tsang J C, Kash J A and Jha S S 1985 *Physica B* **134** 184
- [24] Tsen K T, Kiang J G, Ferry D K and Morkoc H 2006 *Appl. Phys. Lett.* **89** 112111
- [25] Matulionis A 2006 *Phys. Status Solidi* at press